

Supporting Information

Size-dependent electrocatalytic hydrogen evolution activity of arrays of edge-like defects in MoS₂ crystals patterned by focused ion beam

Claudia de Lourenço^{a,b}, Ana B. S. de Araujo^{a,b}, Leonardo H. Hasimoto^{a,d}, Isaque A. A. Feitosa^a, Matheus F. F. das Neves^a, Jefferson Bettini^a, Tarcísio M. Perfecto^a, Tulio C. R. Rocha^c, Thiago J. A. Mori^c, Edson R. Leite^a, Murilo Santhiago^{a,d}*

^a Brazilian Nanotechnology National Laboratory, Brazilian Center for Research in Energy and Materials, Campinas, São Paulo 13083-970, Campinas, Brazil

^b Institute of Chemistry, University of Campinas, Campinas, São Paulo 13083-970, Brazil

^c Brazilian Synchrotron Light Laboratory (LNLS), Brazilian Center for Research in Energy and Materials (CNPEM), 13083-970 Campinas, Brazil

^d Federal University of ABC, Santo André, São Paulo 09210-580, Brazil

*e-mail: murilo.santhiago@lnnano.cnpem.br

S1) Raman spectroscopy

Fig. S1a shows the stereomicroscope images of the MoS₂ pillars and the respective positions where the spectra were collected. Fig. S1b shows the absence of Raman signals for the MoS₂ pillars.

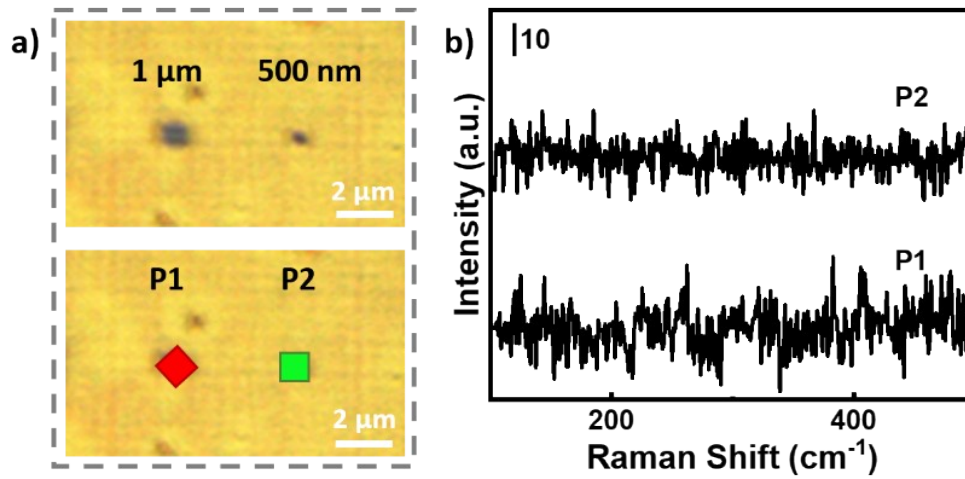


Fig. S1. A) Stereomicroscope images of the pillars. b) Raman spectra.

S2) Single pillar (15×15 μm)

Figs. S2a-b below illustrates the AFM and its respective KPFM image. The height and surface potential profiles are illustrated in Fig. S2c.

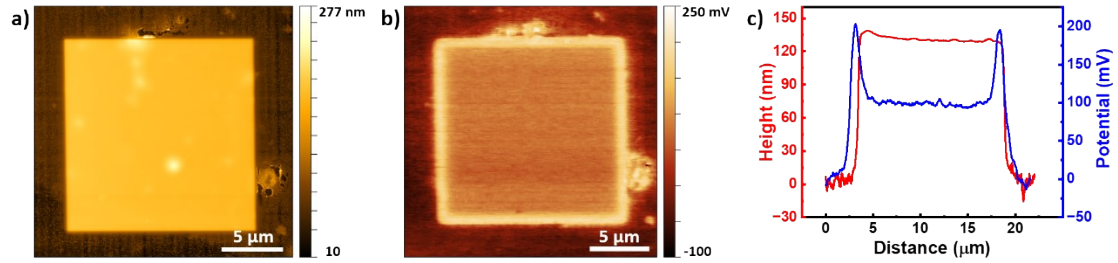


Fig. S2. a) AFM and b) KPFM image obtained for the 15×15 μm wide MoS₂ pillar. c) Height and surface potential profiles.

S3) Survey and High-Resolution XPS

Figure S3a shows the survey spectra obtained in the pristine basal plane (pristine) and at the edges of the pillars (pillar). After the patterning process, the percentage of oxygen in the sample increases by 16% while the S:Mo ratio is close to 2. A shoulder at 531.1 eV in the high-resolution XPS S3b for O1s confirms the presence of Mo-O chemical bonds after the fabrication of the pillars.

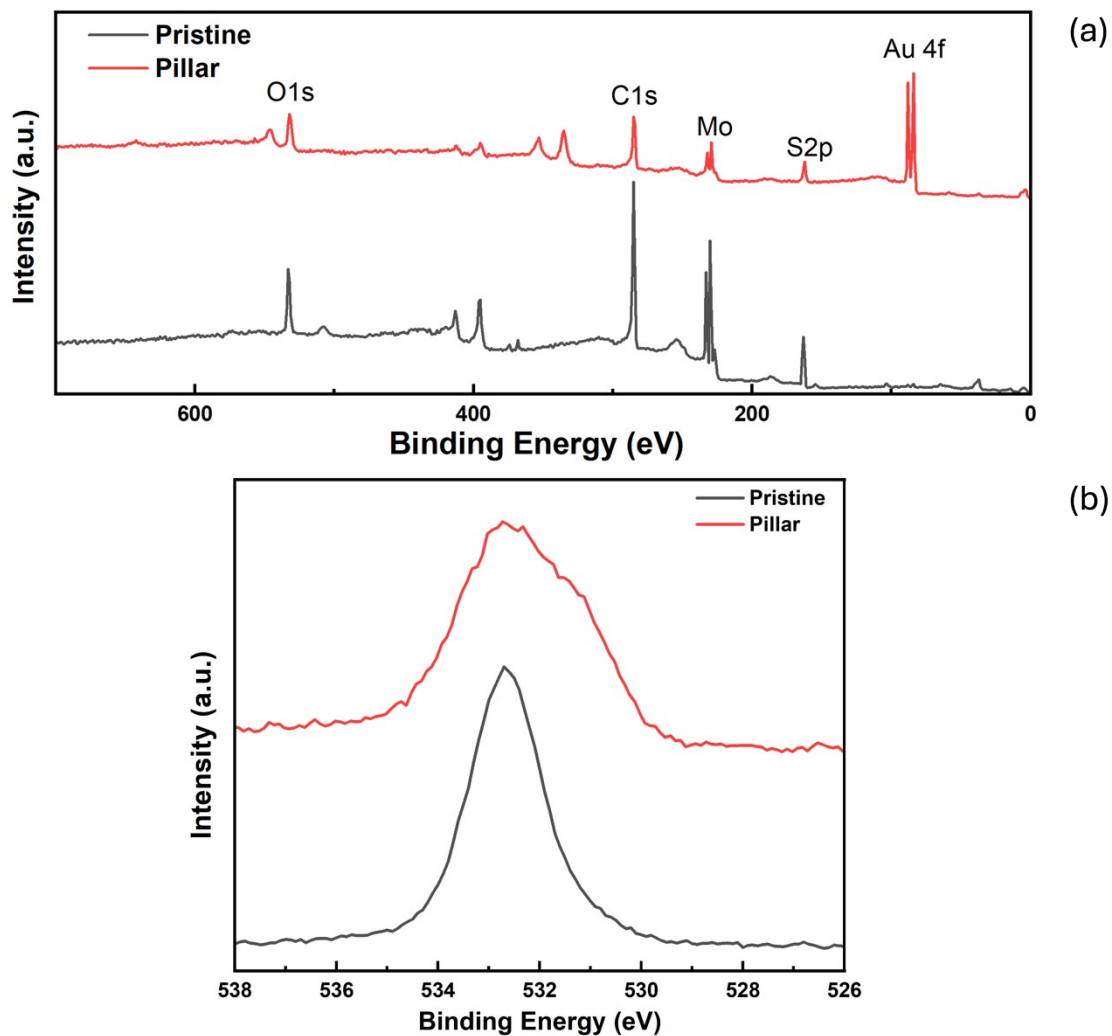


Fig. S3. a) Survey and b) High-resolution XPS for O1s graphs obtained for pristine and single pillar samples.

S4) Raman spectra collected at the edge of the pillar.

The LA mode can be clearly observed in Fig. S3 below. In this case, the spot was positioned close to the edges, as indicated in the manuscript.

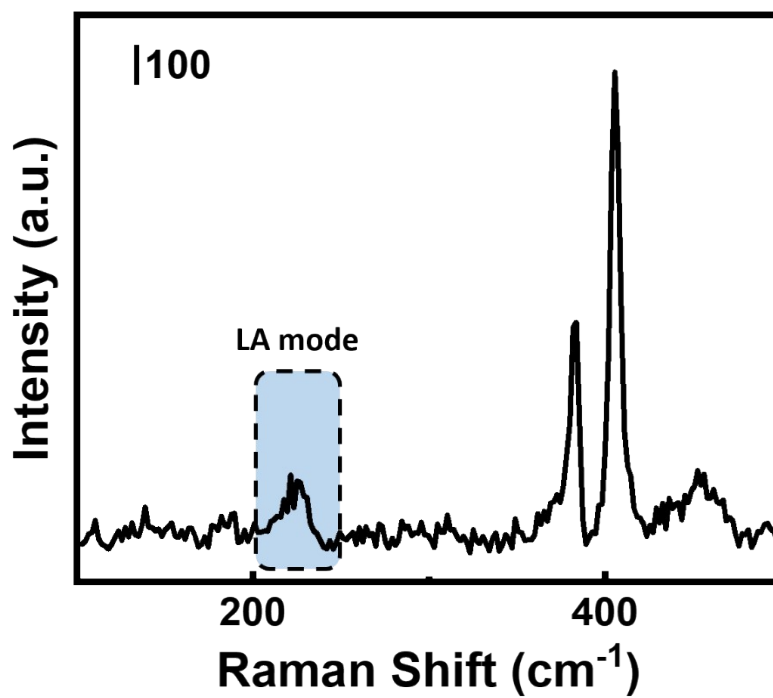


Fig. S4. Raman spectra obtained at the edge of the pillar after electrochemical measurements.

S5) ECSA for different pillar sizes

The electrochemically active surface area (ECSA) was estimated using cyclic voltammetry in the non-faradaic range, with scan rates between 0.05 and 0.09 V s⁻¹. A 0.5 M H₂SO₄ solution (Sigma-Aldrich, SP, Brazil) was used as the supporting electrolyte, purged with N₂ for 1 hour before experiments. The double-layer capacitance was calculated as the average slope from linear fits of the data. Using a specific capacitance of 40 μF cm⁻², the ECSA was determined and inserted in the Figure S5.

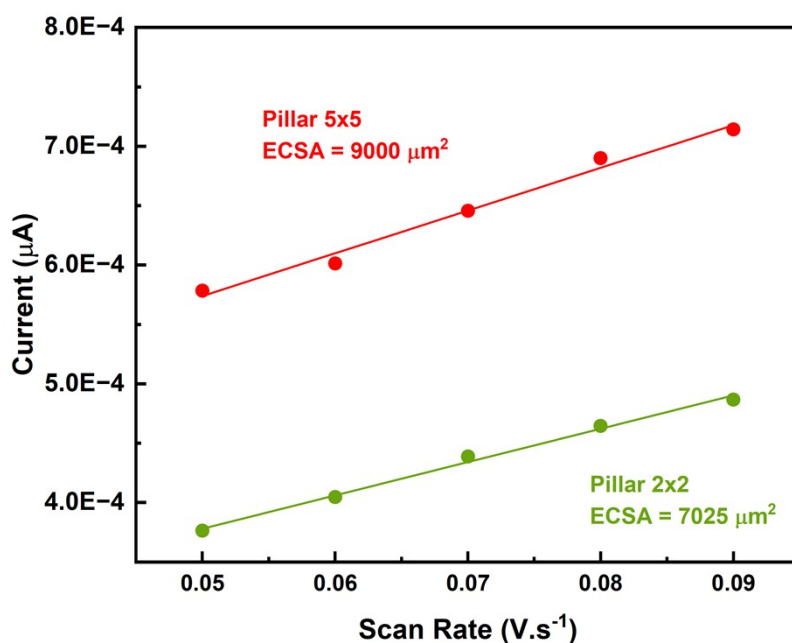


Fig. S5. Current ($\Delta I/2$) vs. scan rate curves for 5x5 and 2x2 μm pillars, and the ECSA for each sample is indicated in the graph. When analyzing the ECSA, it is noticeable that the smaller pillars, which show signs of corrosion, have a reduced active area for HER. This decrease in ECSA negatively impacts the electrocatalytic activity.

S6) Single pillar before and after HER cycles

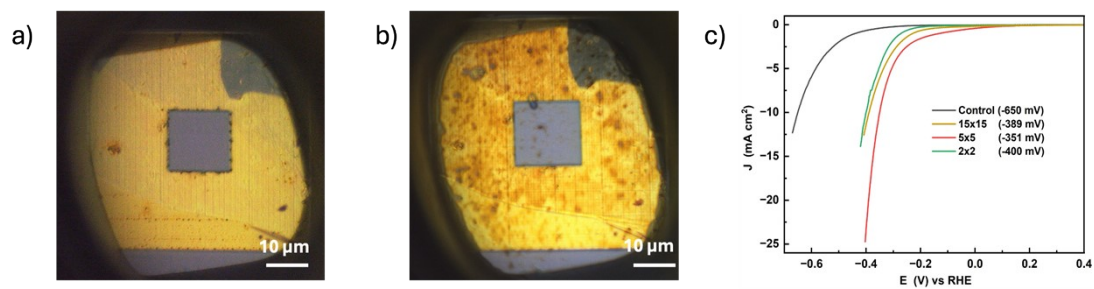


Fig. S6. Single pillar before (a) and after (b) HER process. It is possible to note that the edges remain intact, while the smaller pillars present edge corrosion noticeable in the figures from the main file. Figure c) indicates HER comparing the samples.

S7) Stability tests

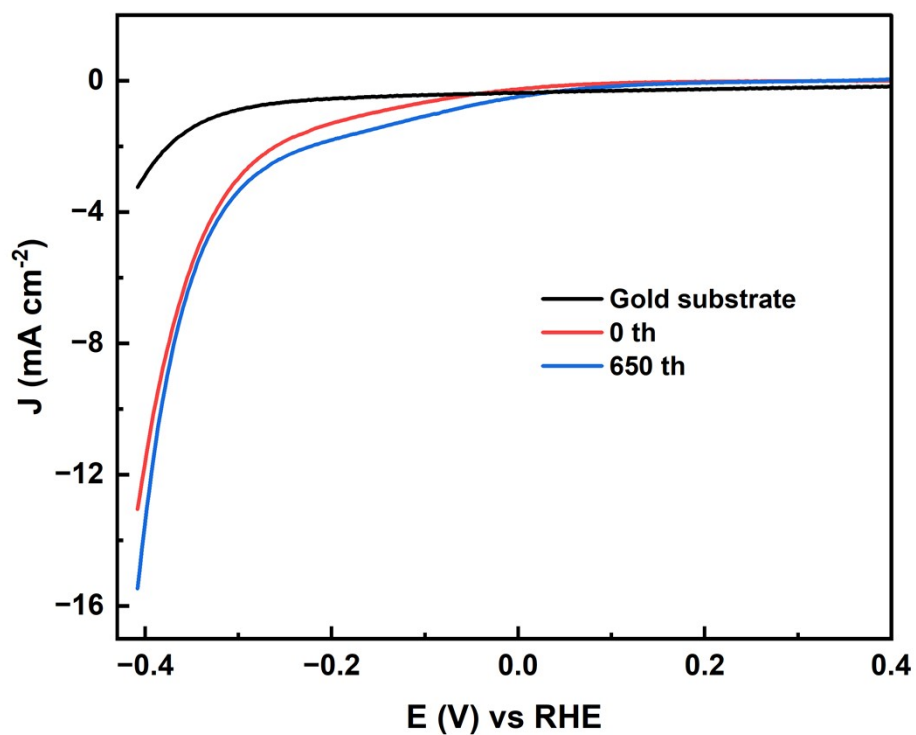


Fig. S7. Stability test of $5 \times 5 \mu\text{m}$ pillars and gold substrate was added for further assessment. The curves indicate stability after 650 HER cycles with a cathodic shift of 33 mV compared to the initial measurements described in the main manuscript file.